Preoperative prediction of microvascular invasion classification in hepatocellular carcinoma based on clinical features and MRI parameters

MING-GE LI[1], YA-NAN ZHANG[2], YING-YING HU[3], LEI LI[2] and HAI-LIAN LYU[2]

[1]Department of Radiology, Tianjin Third Central Hospital, Tianjin 300170, P.R. China;
[2]Department of Radiology, Shengli Oilfield Central Hospital, Dongying, Shandong 257034, P.R. China;
[3]Department of Pathology, Shengli Oilfield Central Hospital, Dongying, Shandong 257034, P.R. China

Received January 29, 2024; Accepted April 17, 2024

DOI: 10.3892/ol.2024.14443

Abstract. Microvascular invasion (MVI) in hepatocellular carcinoma (HCC) is a critical pathological factor and the degree of MVI influences treatment decisions and patient prognosis. The present study aimed to predict the MVI classification based on preoperative MRI features and clinical parameters. The present retrospective cohort study included 150 patients (training cohort, n=108; validation cohort, n=42) with pathologically confirmed HCC. Clinical and imaging characteristics data were collected from Shengli Oilfield Central Hospital (Dongying, China). Univariate and multivariate logistic regression analyses were conducted to assess the association of clinical variables and MRI parameters with MVI (grade M1 and M2) and the M2 classification. Nomograms were developed based on the predictive factors of MVI and the M2 classification. The discrimination capability, calibration and clinical usefulness of the nomograms were evaluated. Multivariate analysis revealed an association between the *Lens culinaris* agglutinin-reactive fraction of α-fetoprotein, protein induced by vitamin K absence-II and tumor margin and MVI-positive status, while peritumoral enhancement and tumor size were demonstrated to be marginal predictors, but were also included in the nomogram. However, among MVI-positive patients, only peritumoral hypointensity and tumor size were demonstrated to be risk factors for the M2 classification. The nomograms, incorporating these variables, exhibited a strong ability to discriminate between MVI-positive and MVI-negative patients with HCC in both the training and validation cohort [area under the curve (AUC), 0.877 and 0.914, respectively] and good performance in predicting the M2 classification in the training and validation cohorts (AUC, 0.720 and 0.782, respectively). Nomograms incorporating clinical parameters and preoperative MRI features demonstrated promising potential as straightforward and effective tools for predicting MVI and the M2 classification in patients with HCC. Such predictive tools could aid in the judicious selection of optimal clinical treatments.

Correspondence to: Dr Hai-Lian Lyu, Department of Radiology, Shengli Oilfield Central Hospital, 31 Jinan Road, Dongying, Dongying, Shandong 257034, P.R. China
E-mail: young-lily@163.com

Key words: hepatocellular carcinoma, microvascular invasion, magnetic resonance imaging, nomogram

Introduction

Hepatocellular carcinoma (HCC) is the most prevalent primary malignant tumor of the liver in Northern and Western Africa and Eastern and South-Eastern Asia, according to statistical data from 2018 (1). Primary curative treatments for HCC include liver resection, radiofrequency ablation and liver transplantation (2). Symptoms of HCC often go unnoticed and early-stage detection remains challenging, leading to missed opportunities for timely surgical intervention upon diagnosis. Furthermore, HCC presents with complex and diverse clinical characteristics (3). Even when small tumors are resected early, long-term survival remains unsatisfactory due to frequent recurrences and metastases (4). Numerous studies have assessed the risk factors associated with early recurrence after surgical resection in patients with HCC. Factors such as large tumor size, elevated serum a-fetoprotein (AFP) levels, microvascular invasion (MVI), poor histological differentiation and Ki-67 expression have been associated with early recurrence in HCC (5-8).

MVI is a histopathological feature that indicates the aggressive behavior of HCC (9). MVI is not detectable through preoperative imaging and its diagnosis relies on the pathology results of tissue specimens obtained during surgery under a microscope (10). MVI involves the infiltration of tumor cells into numerous microvascular structures. Its presence signals the potential for tumor spread and metastasis within the liver, resulting in the formation of a portal vein tumor thrombus or distant metastasis (11). MVI is a risk factor associated with postoperative recurrence and overall survival in patients (12-14), serving as an indicator of a poor prognosis (15). Accurate preoperative evaluation of MVI is required for doctors to determine appropriate treatment strategies for patients (16).

In high-risk patients with MVI, a wide margin of surgical resection is preferred, as it has the potential to improve the prognosis (17).

According to the three-tiered MVI grading system (18), MVI can be classified into three grades: M0, no MVI; M1, 1-5 MVI sites located ≤1 cm away from the tumor surface; or M2, MVI of >5 sites or MVI at >1 cm away from the tumor surface. A recent study identified histological risk classification based on MVI as a valuable prognostic indicator for patients with HCC, revealing an association between grade M2 and a decreased overall survival rate (19). Although previous research has explored MVI prediction, studies on the prediction of MVI grading in patients with HCC with MVI are still limited (5,14,17,19). Chen *et al* (19) assessed MVI classification based on clinical and pathological characteristics as well as CT variables. However, due to the inclusion of pathological factors in this research model, prediction of MVI grading before surgery was not feasible. Therefore, the present study aimed to predict the MVI classification based on preoperative MRI features and clinical parameters, establishing corresponding nomograms to offer guidance for clinicians.

Materials and methods

Ethical approval. The present study was performed according to the ethical standards in the 1964 Declaration of Helsinki. Approval was granted by the Ethics Committee of Shengli Oilfield Central Hospital (approval no. YXLL202400701; Dongying, China) and the requirement for informed consent of patients was waived.

Patients. Two experienced radiologists continuously retrospectively collected data from patients with HCC who underwent liver MRI from the picture archiving and communication system (PACS) of the Shengli Oilfield Central Hospital (Dongying, China). Data from patients between February 2018 and April 2021 were included in the training set. Data from patients between May 2021 and April 2023 were selected for the validation set. The inclusion criteria were as follows: i) Confirmed histopathological diagnosis of HCC with clear grading of MVI; ii) liver MRI examination was performed within 2 weeks before surgical treatment; and iii) presence of single tumors, without invasion of large vessels and distant metastasis. The exclusion criteria were as follows: i) Incomplete MR images or MRI scans with significant artifacts; ii) previous treatment for HCC prior to the latest MRI examination, including hepatectomy, chemotherapy, ablation, immunotherapy, radiofrequency ablation, neoadjuvant chemotherapy, radiotherapy or transcatheter arterial chemoembolization; iii) a history of other malignant tumors; and iv) incomplete clinical or pathological information.

MRI examination. All participants in the present study underwent abdominal MRI using a 3.0 T scanner (MAGNETOM Skyra; Siemens Healthineers) equipped with a phased-array body coil. Before the examination, all patients fasted for 6 h. The sequences of MRI scanning protocol included: i) Fat-suppressed axial T2-weighted imaging; ii) in-phase and out-of-phase axial T1-weighted imaging; iii) diffusion-weighted imaging with b-values of 50 and 800 s/mm^2 with corresponding apparent diffusion coefficient (ADC) maps automatically calculated by the MR system; iv) T1-weighted pre-contrast imaging; and v) dynamic contrast-enhanced imaging. A dose of 0.1 mmol/kg gadoteric acid meglumine (Jiangsu Hengrui Medicine Co., Ltd.) was injected at a rate of 2 ml/sec, followed immediately by a 20-ml physiological saline flush. Hepatic arterial phase, portal venous phase (PVP) and delayed phase images were obtained at 20-30, 70-80 and 180 sec following contrast material injection, respectively.

Clinical, pathological and imaging data analysis. Basic characteristics and clinical laboratory data of patients with HCC were collected from Shengli Oilfield Central Hospital, including age, sex, levels of AFP, *Lens culinaris* agglutinin-reactive fraction of AFP (AFP-L3), protein induced by vitamin K absence-II (PIVKA-II), alanine aminotransferase, aspartate aminotransferase and galactosyl glucosyltransferase, and the presence of cirrhosis and hepatitis B. The pathological report also included additional features such as tumor size on final pathology, histological differentiation and Edmondson-Steiner grades (20).

Two experienced radiologists independently and retrospectively extracted and assessed numerous features from the MR images using the local PACS of the hospital. The radiologists were blinded to clinical and pathological information, and disagreements during image evaluation were resolved through joint consultation and consensus. The evaluated characteristics of the lesions (Fig. S1) included: i) Tumor boundary, clear or unclear; ii) tumor margin, smooth or non-smooth; iii) tumor shape, round, defined as a long diameter/short diameter ratio ≤1.2, or non-round (21); iv) tumor size on MRI, recorded as the maximum diameter of the tumor that was measured in the transverse view on the equilibrium phase (delayed phase) of MRI; v) peritumoral enhancement, defined as presence of enhancement in the peritumoral region during the arterial phase; vi) peritumoral hypointensity, defined as hypointensity in the peritumoral region during the PVP or delayed phase; and vii) ADC value, calculated using regions of interest (30-500 mm^2) placed at the level of the maximum diameter of the lesion and inside the visually perceived lowest portions of the tumors on the ADC maps. Notably, areas characterized by hemorrhagic, cystic, necrotic and calcification features were excluded. The final ADC value was computed as the mean of measurements independently obtained by two radiologists.

Statistical analysis. Statistical analysis was performed using SPSS software (v. 17.0; SPSS, Inc.) and R 4.3.0 (https://www.r-project.org. org/). $P<0.05$ was considered to indicate a statistically significant difference. The accordance of quantitative measurements of observers was evaluated using Intraclass Correlation Coefficient (ICC) analysis, and Cohen's κ analysis was used to assess agreement on MRI features between observers. The defined outcomes for accordance were as follows: Substantial agreement >0.60 and almost perfect agreement >0.80. Continuous variables are presented as either the mean ± standard deviation or median (interquartile range) and were analyzed using the unpaired Student's t-test or the Mann-Whitney U test, depending on the data distribution. Categorical variables are presented as numbers (percentages) and were analyzed using the χ^2 or Fisher's exact test. To identify

potential variables significantly associated with MVI-positive HCC or the M2 classification, an initial univariate analysis was conducted to screen for relevant factors. Variables with P<0.05 in the univariate analysis were considered as candidates and included in the multivariate analysis. The multivariate analysis aimed to determine independent predictors of MVI or the M2 classification.

Nomograms were developed using the predictors that were determined by multivariate logistic regression analysis. These nomograms functioned as graphical aids for predicting MVI-positive HCC or the M2 classification. The predictive performances of the models were assessed in the training cohort and then validated in the validation cohort. Receiver operating characteristic (ROC) curves were generated and the area under the curve (AUC) was calculated with a 95% CI. Internal validation of the models was performed using 1,000 bootstrap samples to decrease the overfit bias. The agreement between the predicted MVI-positive and M2-classified samples based on the model and actual observed frequencies was assessed using the Hosmer-Lemeshow (H-L) test and calibration curve analyses. These evaluations were instrumental in gauging how well the predictions of the model aligned with the observed outcomes. Furthermore, the clinical application values of the nomograms were evaluated using decision curve analysis (DCA) and clinical impact curve (CIC) analysis. DCA involved calculating the net benefits at varying threshold probabilities, providing insights into the potential clinical use of the nomogram. Simultaneously, the CIC was evaluated to understand the overall impact of implementing the nomogram in clinical practice.

Results

Patient characteristics. A total of 150 patients were ultimately selected for analysis, and divided into the training cohort (n=108, age, 63.30±9.81 years) and the validation cohort (n=42, age, 62.69±9.48 years) (Fig. 1). The training cohort included 85 male patients and 23 female patients, with a mean age of 63.30±9.81 years. Of the included patients, 75 (69.4%) presented with MVI-positive HCC and 33 (30.6%) presented with MVI-negative HCC (M0). Among the MVI-positive cases, 25 (33.3%) were classified as M2 grade, signifying a higher degree of invasion, and 50 (66.7%) were classified as M1 grade. The validation cohort included 35 male patients and 7 female patients, with a mean age of 62.69±9.48 years. In this cohort, 30 patients (71.4%) were MVI-positive and 12 patients (28.6%) were MVI-negative (M0). Among the MVI-positive patients, 11 (36.7%) were classified as M2 grade, indicating a higher degree of invasion, whereas 19 (63.3%) were classified as M1 grade. No significant differences were observed between the training and validation cohorts for any variables listed in Table SI (all P>0.05).

The inter-observer reproducibility levels for all MRI parameters were deemed almost perfect and in substantial agreement, with an ICC >0.8 and Cohen's κ >0.70 (Tables SII and SIII). These results indicated a lack of notable systematic differences between observers in the assessment of the MRI parameters. Detailed baseline characteristics, pathological data and MRI variables of the patients in the training cohort are shown in Table I.

In the training cohort, when compared with MVI-negative patients, MVI-positive patients were demonstrated to have significantly higher serum AFP-L3 levels, increased PIVKA-II levels, a higher number of samples with a non-smooth tumor margin, lower ADC values, larger tumor size on MRI, higher levels of peritumoral enhancement and peritumoral hypointensity, larger tumor size on final pathology, lower histological differentiation, and higher Edmondson grades (P<0.05). Furthermore, in the training cohort, patients with M2 grade MVI, when compared with patients with M1 grade MVI, had significantly larger tumor size on MRI, higher levels of peritumoral hypointensity and a larger tumor size on final pathology (P<0.05).

Predictor selection. In the training cohort, several significant independent predictors of MVI-positivity were identified, including AFP-L3 levels [odds ratio (OR), 0.21; 95% CI, 0.07-0.64; P=0.006], PIVKA-II levels (OR, 0.33; 95% CI, 0.11-0.99; P=0.047) and tumor margin (OR, 0.17; 95% CI, 0.03-0.97; P=0.046). Furthermore, larger tumor size on MRI (OR, 2.70; 95% CI, 0.75-9.77; P=0.085) and peritumoral enhancement (OR, 1.30; 95% CI, 0.97-1.75; P=0.129) were notable predictors (Tables II and III). These variables were used to construct corresponding nomograms.

Among patients with MVI-positive HCC in the training cohort, only peritumoral hypointensity (OR, 5.38; 95% CI, 1.21-23.96; P=0.027) and larger tumor size on MRI (OR, 1.16; 95% CI, 1.00-1.34; P=0.048) were significant independent predictors of the M2 classification (Tables II and III). Notably, the present study aimed to predict MVI or the M2 classification in a non-invasive manner. Therefore, risk factors related to pathological indicators associated with MVI or the M2 classification were not analyzed.

Development and validation of nomograms. The MVI-positive nomogram incorporated five features: AFP-L3, PIVKA-II, tumor margin, tumor size on MRI and peritumoral enhancement (Fig. 2A). ROC analysis was performed to assess the discriminative capability of the nomograms. The AUC for the MVI-positive nomogram was 0.877 (95% CI, 0.81-0.94) in the training cohort and 0.914 (95% CI, 0.74-0.99) in the validation cohort (Fig. 3A and B). Furthermore, the bootstrapped calibration curves, which evaluated the consistency between the predicted probability and the actual observed results of the model, were produced for the training cohort and the validation cohort. The calibration curves also demonstrated good consistency in the training and validation cohorts, as indicated by the H-L test (P=0.693 and P=0.703, respectively) with a mean absolute error of 0.026 for the training cohort (Fig. 3C) and 0.05 for the validation cohort (Fig. 3D).

DCA results indicated that, for almost all threshold probabilities, both nomogram models provided a consistently greater overall net benefit compared with intervening in all or none of the patients (Fig. S2A and B). This suggested that the nomograms had practical value in guiding clinical decision-making. The CIC results demonstrated that, at different threshold probabilities within a given population, the predicted number of patients at high risk matched well with the actual number of patients who were indeed at high risk (as indicated by the proximity of the red solid line to the blue dashed line).

This indicated that the nomogram models exhibited notable predictive power, effectively identifying patients at a high risk for the MVI classification (Fig. S2C and D).

The M2 classification nomogram integrated two variables, peritumoral hypointensity and tumor size on MRI (Fig. 2B). The AUC for the M2 classification nomogram was 0.720 (95% CI, 0.60-0.85) in the training cohort (Fig. 4A) and 0.782 (95% CI, 0.61-0.96) in the validation cohort (Fig. 4B). The calibration curves demonstrated good consistency in both cohorts, confirmed by the H-L test (P=0.747 and P=0.406, respectively) with a mean absolute error of 0.065 for the training cohort (Fig. 4C) and 0.115 for the validation cohort (Fig. 4D). DCA results indicated that, for almost all threshold probabilities, both nomogram models provided a consistently greater overall net benefit compared with intervening in all or none of the patients (Fig. S3A and B). The CIC results demonstrated that, at different threshold probabilities within a given population, the predicted number of patients at high risk matched well with the actual number of patients who were indeed at high risk (as indicated by the proximity of the red solid line to the blue dashed line) (Fig. S3C and D). DCA and CIC results indicated that the nomogram models possessed notable predictive power and could effectively identify patients at high risk for the M2 classification (Fig. S3).

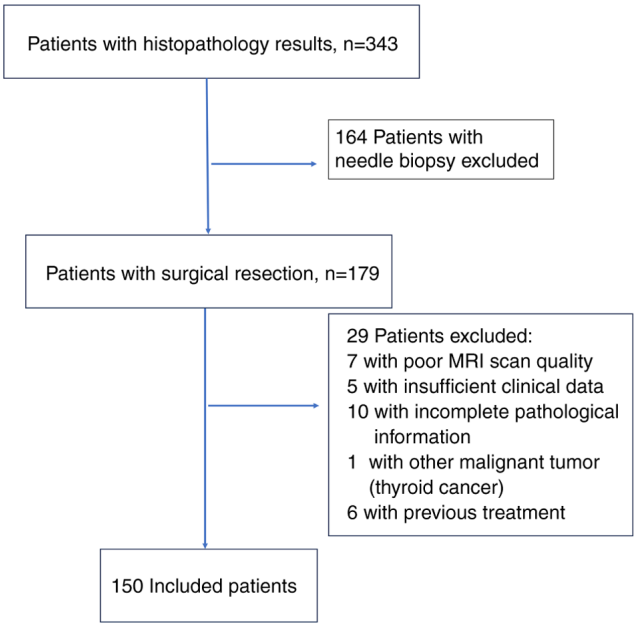

Figure 1. Patient selection flowchart.

Discussion

In the present study, nomogram models capable of preoperatively predicting MVI-positivity and its M2 classification in patients with HCC were developed. These models incorporated both clinical variables and preoperative MRI features, and demonstrated strong performance in predicting MVI status, with AUC values ranging between 0.700 and 0.920, consistent with previous findings (19,21,22). A notable advantage of the present nomogram model is its reliance on relatively simple and easily obtainable clinical parameters and MRI features. Relying on neither complex software nor post-processing techniques, these tools are convenient for doctors to use in their practice. The inclusion of accessible variables enhances the practicality and feasibility of integrating these models into the routine clinical workflow. Overall, the present study provided promising tools for the preoperative prediction of MVI-positive status and the M2 classification in patients with HCC, offering clinicians information for treatment planning and decision-making.

MVI is a marker for assessing the invasive behavior, recurrence and metastasis of HCC (22,23). Its presence affects the prognosis of patients (24). Grading the risk of MVI through preoperative assessment can aid doctors in making more informed treatment decisions. Previous studies have highlighted that severe MVI classification or M2 grade is a valuable predictor of prognosis in patients (19,24). Furthermore, Hwang *et al* (24) reported that severe MVI is associated with lower survival rates and more aggressive tumor behavior. By contrast, there was no significant difference in survival rates between patients with mild MVI and patients with no MVI. Xu *et al* (25) reported no notable disparity in early recurrence after curative resection between patients with M0 HCC and patients with M1 HCC; however, the M2 grade was potentially associated with a poorer prognosis in patients with HCC. Although numerous studies (6,7,19,21,22,26-28) have focused on predicting MVI status in patients with HCC, few have explored the preoperative grading of M2. To the best of our knowledge, no previous attempts have been made to use clinical and MRI features for preoperative prediction of the M2 classification in patients with HCC. Most studies have primarily concentrated solely on predicting the occurrence of MVI (6,7,21,26-28) or establishing classification models using enhanced CT radiomics features and pathological characteristics (19,22). To the best of our knowledge, there have been no previous studies using MRI features to non-invasively predict M2 classification in patients with HCC. Therefore, the present study represents advancement by developing reliable nomograms based on MRI features for the preoperative prediction of the M2 grade in patients with MVI-positive HCC.

Previous studies have compared the predictive abilities of CT and MRI for MVI in HCC, indicating that they have a comparable predictive performance (29,30), with the MRI model exhibiting a slightly higher AUC compared with the CT model (29). Currently, to the best of our knowledge, no studies have directly compared the uses of CT and MRI in predicting the MVI classification. Notably, the MRI variables (peritumoral hypointensity and tumor size) used for MVI classification in the present study differed from the CT variable (tumor margin) mentioned in the Chen *et al* (19) study but are consistent with the Zheng *et al* (22) study. These disparities may be attributed to differences in the study samples. Therefore, future research should use the same samples to more accurately compare the predictive performance of the two imaging modalities for MVI classification.

Previous studies have reported associations between clinical and imaging variables, such as AFP-L3, PIVKA-II, tumor size, peritumoral enhancement, non-smooth tumor margin and peritumoral hypointensity, and MVI in patients with HCC (5,19,22,24,31-33). The present study also demonstrated that high levels of AFP-L3, PIVKA-II and non-smooth tumor

Table I. Baseline characteristics of patients with HCC in the training cohort.

Characteristics	All patients with HCC			Patients with MVI-positive HCC		
	MVI-positive (n=75)	MVI-negative (n=33)	P-value	M2 grade (n=25)	M1 grade (n=50)	P-value
Sex[b]			0.600			0.697
Male	58 (77.3)	27 (81.8)		20 (80.0)	38 (76.0)	
Female	17 (22.7)	6 (18.2)		5 (20.0)	12 (24.0)	
Age[a], years	62.88±9.57	64.24±10.43	0.509	62.24±9.14	63.20±9.85	0.685
AFP[b], ng/ml			0.417			0.348
≤400	56 (74.7)	27 (81.8)		17 (68.0)	39 (78.0)	
>400	19 (25.3)	6 (18.2)		8 (32.0)	11 (22.0)	
AFP-L3[b], %			<0.001			0.126
≤10	27 (36.0)	26 (78.8)		6 (24.0)	21 (42.0)	
>10	48 (64.0)	7 (21.2)		19 (76.0)	29 (58.0)	
PIVKA-II[b], mAU/ml			<0.001			>0.999
≤40	10 (13.3)	17 (51.5)		3 (12.0)	7 (14.0)	
>40	65 (86.7)	16 (48.5)		22 (88.0)	43 (86.0)	
Hepatitis B[b]			0.101			0.356
Yes	64 (85.3)	32 (97.0)		20 (80.0)	44 (88.0)	
No	11 (14.7)	1 (3.0)		5 (20.0)	6 (12.0)	
Cirrhosis[b]			0.576			0.834
Yes	61 (81.3)	29 (87.9)		20 (80.0)	41 (82.0)	
No	14 (18.7)	4 (12.1)		5 (20.0)	9 (18.0)	
ALT[a], U/l	29.0 (19.0)	26.0 (21.5)	0.237	34.0 (24.0)	28.0 (16.0)	0.125
AST[a], U/l	27.0 (23.0)	25.0 (22.0)	0.371	27.0 (24.5)	27.0 (23.5)	0.589
GGT[a], U/l	40.0 (67.0)	50.0 (70.0)	0.535	62.0 (82.5)	39.0 (40.25)	0.132
Tumor boundary[b]			0.053			0.172
Clear	58 (77.3)	31 (93.9)		17 (68.0)	41 (82.0)	
Unclear	17 (22.7)	2 (6.1)		8 (32.0)	9 (18.0)	
Tumor shape[b]			0.090			0.215
Round	52 (69.3)	28 (84.8)		15 (60.0)	37 (74.0)	
Non-round	23 (30.7)	5 (15.2)		10 (40.0)	13 (26.0)	
Tumor margin[b]			<0.001			0.071
Smooth	41 (54.7)	31 (93.9)		10 (40.0)	31 (62.0)	
Non-smooth	34 (45.3)	2 (6.1)		15 (60.0)	19 (38.0)	
ADC[a], mm^2/sec	0.9 (0.2)	1.0 (0.3)	0.027	0.9 (0.2)	0.9 (0.3)	0.774
Tumor size on MRI[a], cm	4.6 (5.5)	2.6 (2.6)	<0.001	6.2 (7.05)	4.1 (3.05)	0.008
Peritumoral enhancement[b]			<0.001			0.198
Yes	40 (53.3)	5 (15.2)		16 (64.0)	24 (48.0)	
No	35 (46.7)	28 (84.8)		9 (36.0)	26 (52.0)	
Peritumoral hypointensity[b]			0.017			0.005
Yes	11 (14.7)	0 (0.0)		8 (32.0)	3 (6.0)	
No	64 (85.3)	33 (100.0)		17 (68.0)	47 (94.0)	
Tumor size measured by pathology[a], cm	5.0 (5.0)	3.0 (2.8)	<0.001	6.0 (7.0)	4.6 (3.5)	0.049
Histological differentiation[b]			<0.001			>0.999
Low/middle	74 (98.7)	22 (66.7)		25 (100.0)	49 (98.0)	
High	1 (1.3)	11 (33.3)		0 (0.0)	1 (2.0)	
Edmondson-Steiner grade[b]			0.009			0.624
I-II	39 (52.0)	26 (78.8)		14 (56.0)	25 (50.0)	
III-IV	36 (48.0)	7 (21.2)		11 (44.0)	25 (50.0)	

[a]Continuous variables are presented as the mean ± SD or median (interquartile range), [b]categorical variables are presented as n (%). ADC, apparent diffusion coefficient; AFP, α-fetoprotein; AFP-L3, *Lens culinaris* agglutinin-reactive fraction of AFP; ALT, alanine aminotransferase; AST, aspartate aminotransferase; GGT, galactosyl glucosyltransferase; HCC, hepatocellular carcinoma; MVI, microvascular invasion; PIVKA-II, protein induced by vitamin K absence-II.

Table II. Univariate logistic regression analysis for the prediction of MVI-positivity and the M2 classification in the training cohort.

	MVI-positive		M2 classification	
Variable	OR (95% CI)	P-value	OR (95% CI)	P-value
Sex	0.76 (0.27-2.14)	0.601	1.26 (0.39-4.09)	0.697
Age, years	0.99 (0.95-1.03)	0.505	0.99 (0.94-1.04)	0.680
AFP, ng/ml	0.66 (0.24-1.83)	0.419	0.60 (0.21-1.76)	0.350
AFP-L3, %	0.15 (0.06-0.40)	<0.001	0.44 (0.15-1.28)	0.131
PIVKA-II, mAU/ml	0.15 (0.06-0.38)	<0.001	0.84 (0.20-3.56)	0.810
Hepatitis	0.18 (0.02-1.47)	0.110	0.55 (0.15-2.00)	0.360
Cirrhosis	0.60 (0.18-1.99)	0.404	0.88 (0.26-2.97)	0.834
ALT, U/l	1.00 (0.99-1.00)	0.381	1.00 (0.99-1.02)	0.629
AST, U/l	1.00 (0.99-1.00)	0.340	1.00 (0.99-1.02)	0.964
GGT, U/l	1.00 (0.99-1.00)	0.984	1.00 (0.99-1.01)	0.178
Tumor boundary	0.22 (0.05-1.02)	0.052	0.47 (0.15-1.41)	0.177
Tumor shape	0.40 (0.14-1.18)	0.097	0.53 (0.19-1.46)	0.218
Tumor margin	0.08 (0.02-0.35)	0.001	0.41 (0.15-1.09)	0.074
ADC, mm^2/sec	0.11 (0.01-0.09)	0.059	0.47 (0.02-8.74)	0.613
Tumor size on MRI	1.48 (1.17-1.88)	0.001	1.20 (1.04-1.38)	0.010
Peritumoral enhancement	6.40 (2.23-18.37)	0.001	1.93 (0.72-5.17)	0.193
Peritumoral hypointensity	$8.33x10^8$ (0.00-Infinity)	0.999	7.37 (1.75-31.06)	0.006

AFP, α-fetoprotein; AFP-L3, *Lens culinaris* agglutinin-reactive fraction of AFP; ADC, apparent diffusion coefficient; ALT, alanine aminotransferase; AST, aspartate aminotransferase; GGT, galactosyl glucosyltransferase; MVI, microvascular invasion; OR, odds ratio; PIVKA-II, protein induced by vitamin K absence-II.

Table III. Multivariate logistic regression analysis for the prediction of MVI-positivity and the M2 classification in the training cohort.

	MVI-positive		M2 classification	
Variable	OR (95% CI)	P-value	OR (95% CI)	P-value
AFP-L3, %	0.21 (0.07-0.64)	0.006	-	-
PIVKA-II, mAU/ml	0.33 (0.11-0.99)	0.047	-	-
Tumor margin	0.17 (0.03-0.97)	0.046	-	-
Tumor size on MRI	2.70 (0.75-9.77)	0.085	1.16 (1.00-1.34)	0.048
Peritumoral enhancement	1.30 (0.97-1.75)	0.129	-	-
Peritumoral hypointensity	-	-	5.38 (1.21-23.96)	0.027

AFP-L3, *Lens culinaris* agglutinin-reactive fraction of α-fetoprotein; MVI, microvascular invasion; OR, odds ratio; PIVKA-II, protein induced by vitamin K absence-II.

margin were significant risk factors for MVI. Furthermore, peritumoral hypointensity and tumor size were significantly associated with the M2 classification, which is consistent with previous research findings (22). Furthermore, AFP-L3 is a specific subtype of AFP that is produced by malignant hepatocytes (34) and has rarely been included in previous models. Nevertheless, several studies have identified AFP-L3 as an independent risk factor for predicting early recurrence of HCC (35,36). Furthermore, AFP-L3 has been reported to reflect poor histological differentiation and unfavorable tumor behavior, such as early vascular invasion, rapid growth, and intrahepatic and early distant metastasis (32,36). A previous imaging study indicated that AFP-L3-positive HCCs are highly vascularized (37). PIVKA-II, a novel serum marker for HCC widely used in clinical practice, has exhibited higher diagnostic sensitivity and specificity for HCC vascular invasion compared with AFP (38). Wang *et al* (39) reported an association between PIVKA-II (>40 mAU/ml) and early recurrence

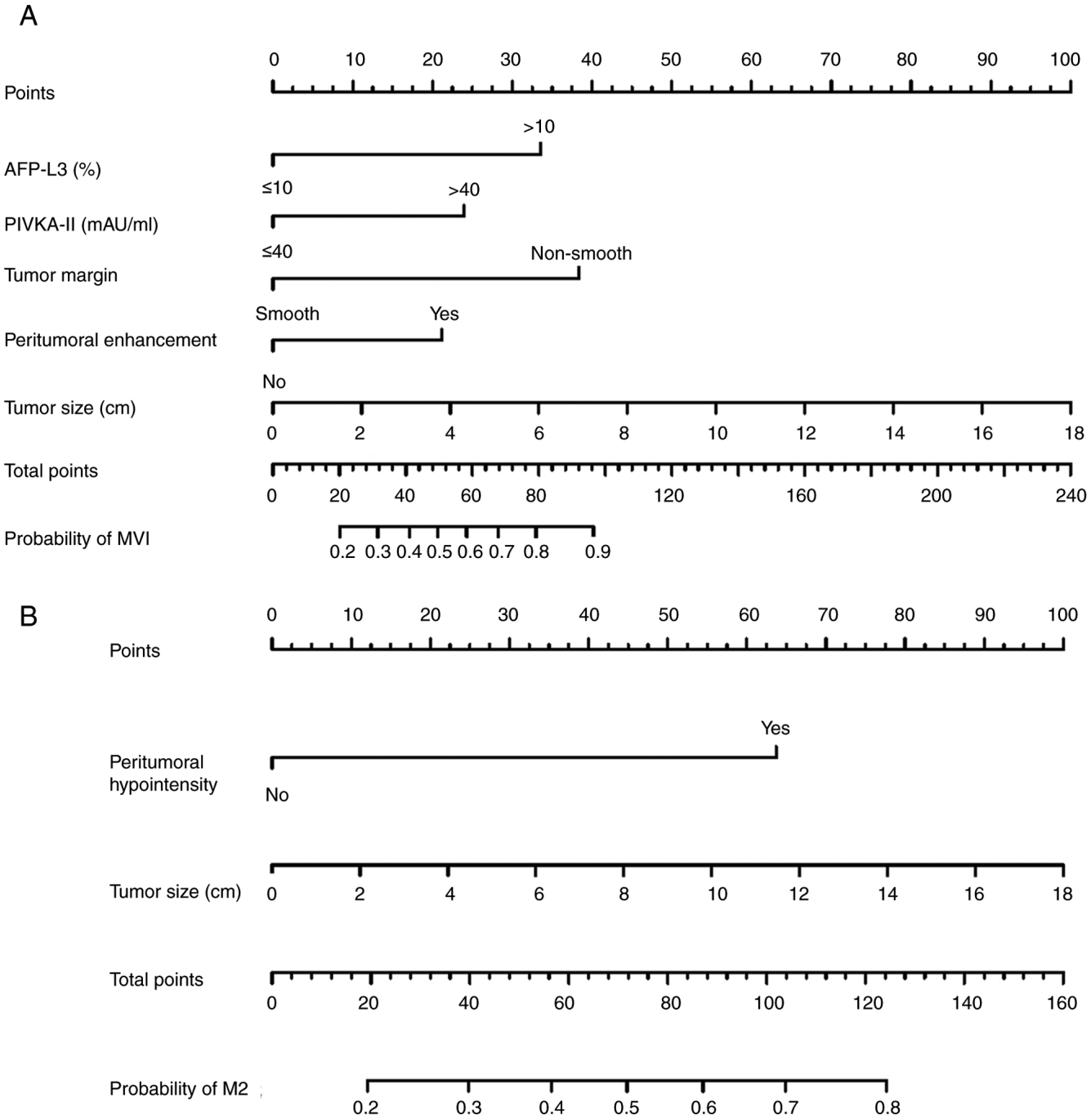

Figure 2. (A) Nomogram for predicting MVI-positivity in patients with hepatocellular carcinoma in the training cohort. (B) Nomogram for predicting M2 grade in patients with MVI-positivity hepatocellular carcinoma in the training cohort. Each variable corresponds to the respective point on the variable axis. A vertical line can be drawn from this point to the ruler above the nomogram to obtain the individual score for this variable. By summing up the scores of each variable, the total score is obtained. The point on the MVI or M2 risk probability axis corresponding to the total score is the corresponding MVI or M2 risk probability of the patient. AFP-L3, *Lens culinaris* agglutinin-reactive fraction of AFP; MVI, microvascular invasion; PIVKA-II, protein induced by vitamin K absence-II.

after HCC resection, identifying it as an independent risk factor for MVI. PIVKA-II has also been demonstrated to be a reliable predictor of MVI and survival in patients with HCC (5). However, in the present study, univariate analysis did not find an association between AFP-L3 levels or PIVKA-II and M2 grade MVI, and there was no significant difference between these two variables in M1 and M2 grading. The distinction between the M1 and M2 grades is defined by the number of MVIs and the distance from the tumor. This implies that the levels of AFP-L3 or PIVKA-II may not directly reflect the number of MVIs or the distance from the tumor, and thus, they may not be directly associated with the M2 classification.

A meta-analysis has highlighted that the non-smooth margin of the tumor imaged preoperatively is an indicator of MVI, suggesting its inclusion in future rating systems (39). Consistently, in the present study, a non-smooth tumor margin was also demonstrated to be a significant risk factor for MVI. This observation can be explained by the fact that

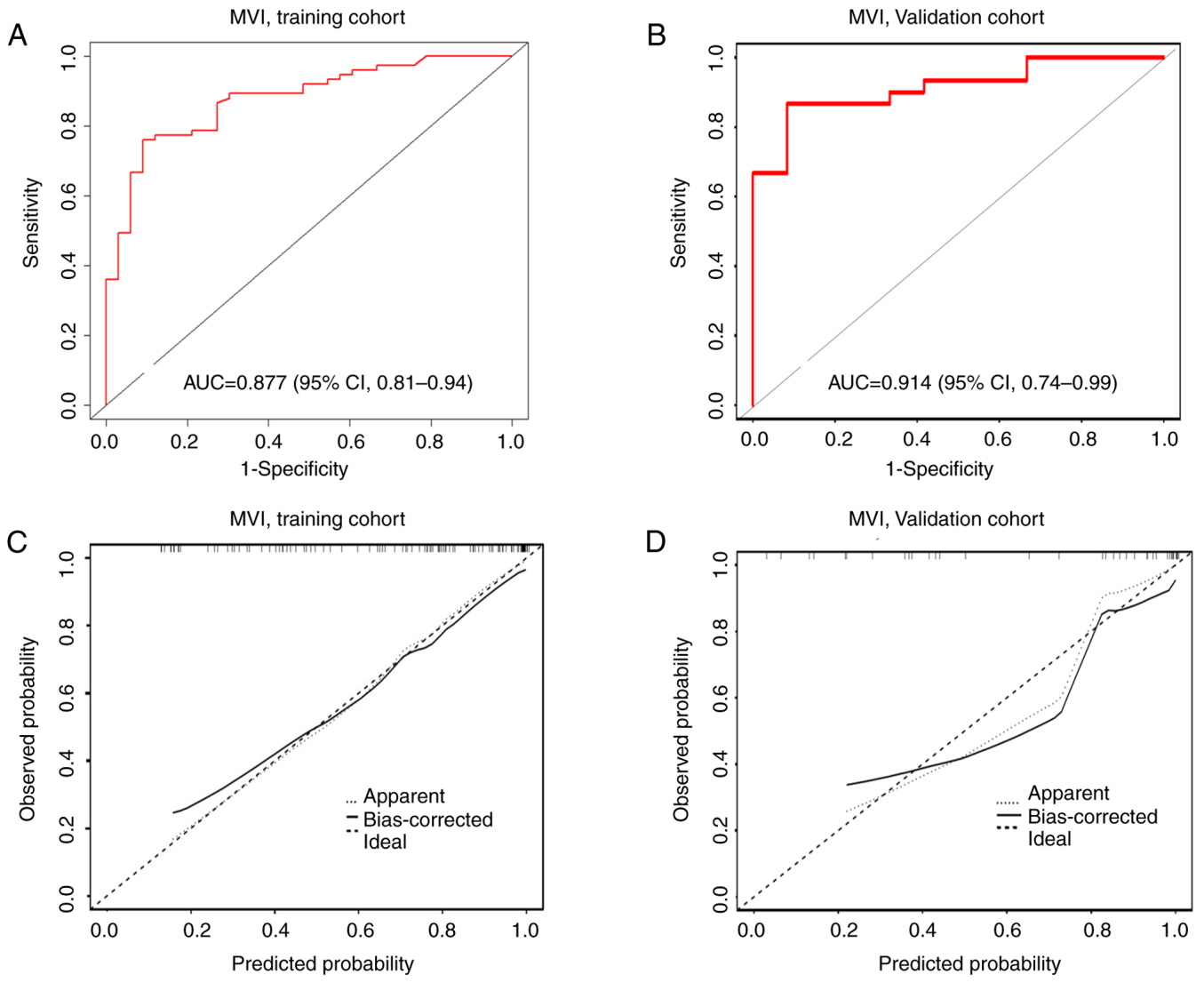

Figure 3. (A) Receiver operating characteristic curve of the MVI nomogram in the training cohort. (B) Receiver operating characteristic curve of the MVI nomogram in the validation cohort. (C) Calibration curves of the MVI nomogram in the training cohort. (D) Calibration curves of the MVI nomogram in the validation cohort. The forecast accuracy of the nomogram improves as the dashed apparent line approaches the diagonal dashed ideal line, and the solid line is bias-corrected. MVI, microvascular invasion.

MVI typically occurs in extra-tumoral extension areas, and irregular tumor margins can indicate the invasive biological behavior of HCC, where infiltration extends from the tumor surface into the hepatic parenchyma (40). Notably, tumor size on MRI and peritumoral enhancement were considered risk factors, as determined by univariate analysis; however, they were not significant independent predictors of MVI in the multivariate analysis. This lack of significance might change with a larger sample size. Despite this, given their association with MVI in previous studies (5,14,17,19,41,42), these factors were included in the nomogram to establish a more comprehensive model. Tumor size was treated as a continuous variable to capture the full range of sizes and minimize information loss, aiming for a comprehensive understanding of its impact on predicting MVI status. A significant difference in tumor size on MRI was observed between patients with M1 grade MVI and patients with M2 grade MVI, consistent with previous research associating larger tumor size with severe MVI (22,39). We hypothesized that tumor size not only affects the ability of tumor cells to invade microvessels but is also linked to the number of MVI sites. However, this association was not identified in a study by Chen *et al* (19), which may be partially due to methodological differences and potential biases in cohort selection. Future studies with larger sample sizes and more comprehensive data analysis methods could provide further insights into the relationship between tumor size and the number of MVI sites.

The results of the multivariate analysis of M2 grade risk factors revealed a significant association between peritumoral hypointensity and the M2 grade. Peritumoral hypointensity may be associated with the invasion of surrounding structures, reflecting hemodynamic perfusion changes in HCC with MVI. Specifically, peritumoral hypointensity is linked to the presence of microscopic tumor thrombi around the tumor, potentially causing small portal vein occlusion (43,44). This occlusion can lead to a decrease or absence of portal vein blood flow, subsequently resulting in hemodynamic changes (43). Although Lee *et al* (43) used a hepatobiliary contrast agent (HBA), a recent

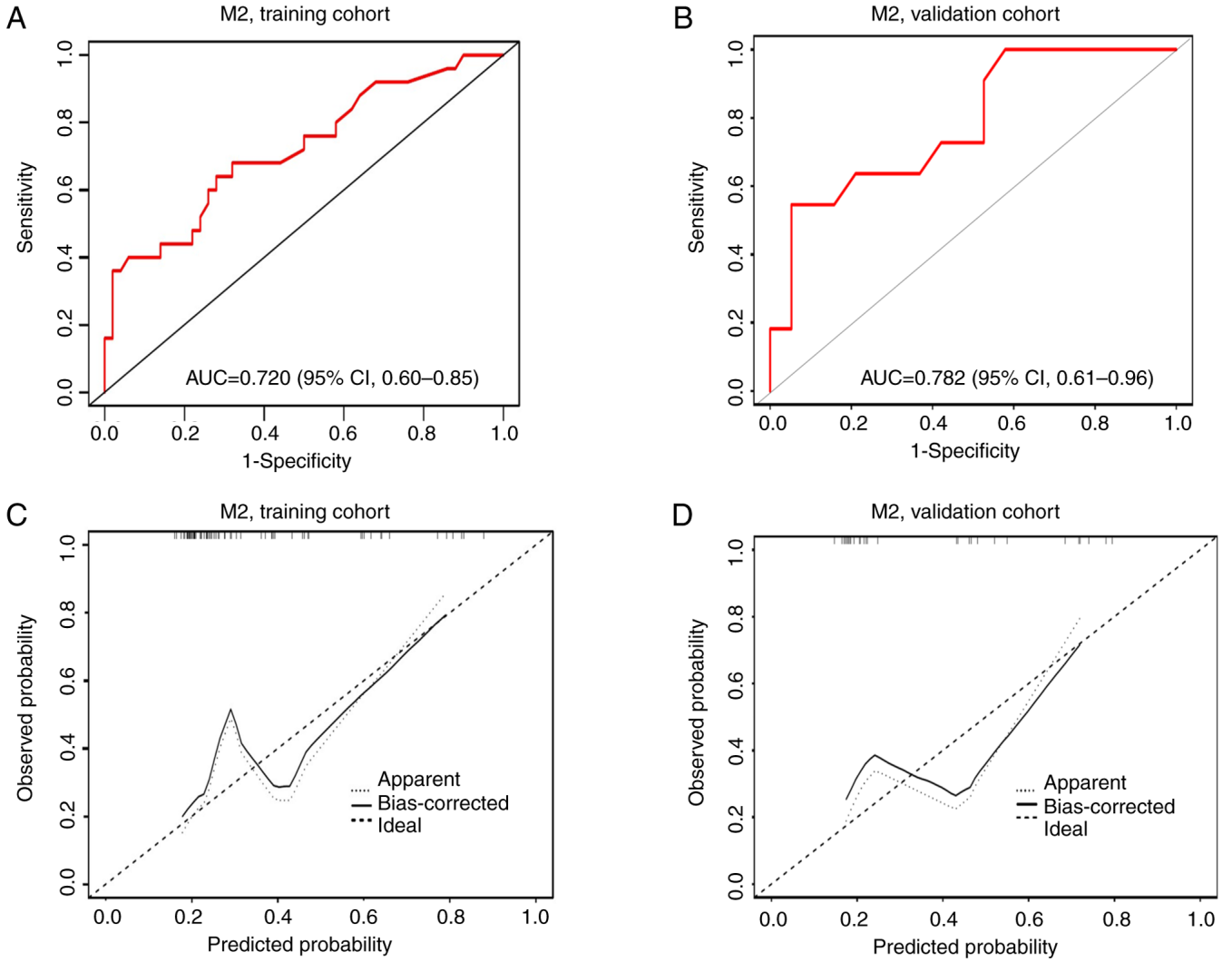

Figure 4. (A) Receiver operating characteristic curve of the M2 grade nomogram in the training cohort. (B) Receiver operating characteristic curve of the M2 grade nomogram in validation cohort. (C) Calibration curves of the M2 grade nomogram in the training cohort. (D) Calibration curves of the M2 grade nomogram in the validation cohort. The forecast accuracy of the nomogram improves as the dashed apparent line approaches the diagonal dashed ideal line, and the solid line is bias-corrected.

study has shown non-HBA specific MRI features, including peritumoral hypointensity in the PVP, may reveal similar pathological changes as the hypointensity of HBA around the tumor (44). However, previous studies have reported inconsistent findings regarding the relationship between MVI and peritumoral hypointensity (14,22,24,33,43). One reason for this may be variations in imaging examination methods and contrast agents used. Another factor may be differences in sample size. Although An *et al* (32) and Lee *et al* (14) reported that the presence of peritumoral hypointensity on hepatobiliary phase images was specific for the diagnosis of MVI in HCC, their studies did not classify MVI into different grades, and thus, the relationship between MVI grading and peritumoral hypointensity remains unconfirmed. As grading of MVI is defined by the number of MVIs and their distance from the tumor, and peritumoral hypointensity is associated with MVI grading, the results of the present study suggested that peritumoral hypointensity affects the number of MVI sites and the distance of MVI from the tumor. However, further large-scale studies using consistent methodologies are required to confirm this association.

The present study had some limitations. Firstly, this was a single-center and relatively small sample size study, and it would be beneficial to conduct larger-scale studies involving multiple centers to validate and further assess the relationships identified. Secondly, the retrospective nature of the present study introduced the possibility of selection bias in case selection. To mitigate this, a continuous case collection approach was used to minimize potential bias. Thirdly, although the present study evaluated the relationship between imaging features and tumor biological behavior, acknowledging that these imaging features may not comprehensively explain the complex underlying mechanisms is crucial. Furthermore, additional research is warranted to further elucidate the underlying biological processes and their association with the demonstrated imaging findings.

In conclusion, the present study developed and validated nomograms that integrate clinical parameters and preoperative MRI features for the prediction of MVI-positivity and the M2 classification in patients with HCC. These nomograms offer noninvasive, straightforward and practical tools to allow clinicians to formulate rational treatment strategies.

Acknowledgements

Not applicable.

Funding

No funding was received.

Availability of data and materials

The data generated in the present study are not publicly available due to use in further studies but may be requested from the corresponding author.

Authors' contributions

HLL designed the study. HLL, YNZ, YYH and LL acquired the patient data. MGL, YYH and HLL analyzed and interpreted the data. MGL and HLL wrote, reviewed and revised the manuscript. HLL and YNZ confirm the authenticity of all the raw data. All authors read and approved the final version of the manuscript.

Ethics approval and consent to participate

The present retrospective study was approved by the Institutional Ethics Committee of the Shengli Oilfield Central Hospital (approval no. YXLL202400701; Dongying, China), which waived the requirement for written informed consent.

Patient consent for publication

Not applicable.

Competing interests

The authors declare that they have no competing interests.

References

1. Bray F, Ferlay J, Soerjomataram I, Siegel RL, Torre LA and Jemal A: Global cancer statistics 2018: GLOBOCAN estimates of incidence and mortality worldwide for 36 cancers in 185 countries. CA Cancer J Clin 68: 394-424, 2018.
2. Earl TM and Chapman WC: Hepatocellular carcinoma: Resection versus transplantation. Semin Liver Dis 33: 282-292, 2013.
3. Chidambaranathan-Reghupaty S, Fisher PB and Sarkar D: Hepatocellular carcinoma (HCC): Epidemiology, etiology and molecular classification. Adv Cancer Res 149: 1-61, 2021.
4. Heimbach JK, Kulik LM, Finn RS, Sirlin CB, Abecassis MM, Roberts LR, Zhu AX, Murad MH and Marrero JA: AASLD guidelines for the treatment of hepatocellular carcinoma. Hepatology 67: 358-380, 2018.
5. Kaibori M, Ishizaki M, Matsui K and Kwon AH: Predictors of microvascular invasion before hepatectomy for hepatocellular carcinoma. J Surg Oncol 102: 462-468, 2010.
6. Wang H, Liu R, Mo H, Li R, Lian J, Liu Q and Han S: A novel nomogram predicting the early recurrence of hepatocellular carcinoma patients after R0 resection. Front Oncol 13: 1133807, 2023.
7. Chen YD, Zhang L, Zhou ZP, Lin B, Jiang ZJ, Tang C, Dang YW, Xia YW, Song B and Long LL: Radiomics and nomogram of magnetic resonance imaging for preoperative prediction of microvascular invasion in small hepatocellular carcinoma. World J Gastroenterol 28: 4399-4416, 2022.
8. Cao Y, Ke R, Wang S, Zhu X, Chen J, Huang C, Jiang Y and Lv L: DNA topoisomerase IIα and Ki67 are prognostic factors in patients with hepatocellular carcinoma. Oncol Lett 13: 4109-4116, 2017.
9. Wang H, Qian YW, Wu MC and Cong WM: Liver resection is justified in patients with BCLC intermediate stage hepatocellular carcinoma without microvascular invasion. J Gastrointest Surg 24: 2737-2747, 2020.
10. Sumie S, Nakashima O, Okuda K, Kuromatsu R, Kawaguchi A, Nakano M, Satani M, Yamada S, Okamura S, Hori M, *et al*: The significance of classifying microvascular invasion in patients with hepatocellular carcinoma. Ann Surg Oncol 21: 1002-1009, 2014.
11. Wang L, Jin YX, Ji YZ, Mu Y, Zhang SC and Pan SY: Development and validation of a prediction model for microvascular invasion in hepatocellular carcinoma. World J Gastroenterol 26: 1647-1659, 2020.
12. Lim KC, Chow PK, Allen JC, Chia GS, Lim M, Cheow PC, Chung AY, Ooi LL and Tan SB: Microvascular invasion is a better predictor of tumor recurrence and overall survival following surgical resection for hepatocellular carcinoma compared to the Milan criteria. Ann Surg 254: 108-113, 2011.
13. Xu X, Zhang HL, Liu QP, Sun SW, Zhang J, Zhu FP, Yang G, Yan X, Zhang YD and Liu XS: Radiomic analysis of contrast-enhanced CT predicts microvascular invasion and outcome in hepatocellular carcinoma. J Hepatol 70: 1133-1144, 2019.
14. Lee S, Kim SH, Lee JE, Sinn DH and Park CK: Preoperative gadoxetic acid-enhanced MRI for predicting microvascular invasion in patients with single hepatocellular carcinoma. J Hepatol 67: 526-534, 2017.
15. Lei Z, Li J, Wu D, Xia Y, Wang Q, Si A, Wang K, Wan X, Lau WY, Wu M and Shen F: Nomogram for preoperative estimation of microvascular invasion risk in hepatitis B virus-related hepatocellular carcinoma within the Milan Criteria. JAMA Surg 151: 356-363, 2016.
16. Ma X, Wei J, Gu D, Zhu Y, Feng B, Liang M, Wang S, Zhao X and Tian J: Preoperative radiomics nomogram for microvascular invasion prediction in hepatocellular carcinoma using contrast-enhanced CT. Eur Radiol 29: 3595-3605, 2019.
17. Chong HH, Yang L, Sheng RF, Yu YL, Wu DJ, Rao SX, Yang C and Zeng MS: Multi-scale and multi-parametric radiomics of gadoxetate disodium-enhanced MRI predicts microvascular invasion and outcome in patients with solitary hepatocellular carcinoma ≤5 cm. Eur Radiol 31: 4824-4838, 2021.
18. Cong WM, Bu H, Chen J, Dong H, Zhu YY, Feng LH and Chen J; Guideline Committee: Practice guidelines for the pathological diagnosis of primary liver cancer: 2015 Update. World J Gastroenterol 22: 9279-9287, 2016.
19. Chen S, Wang C, Gu Y, Ruan R, Yu J and Wang S: Prediction of microvascular invasion and its M2 classification in hepatocellular carcinoma based on nomogram analyses. Front Oncol 11: 774800, 2022.
20. Edmondson HA and Steiner PE: Primary CARCINOMA OF THE LIver: A study of 100 cases among 48,900 necropsies. Cancer 7: 462-503, 1954.
21. Zhang S, Duan C, Zhou X, Liu F, Wang X, Shao Q, Gao Y, Duan F, Zhao R and Wang G: Radiomics nomogram for prediction of microvascular invasion in hepatocellular carcinoma based on MR imaging with Gd-EOB-DTPA. Front Oncol 12: 1034519, 2022.
22. Zheng X, Xu YJ, Huang J, Cai S and Wang W: Predictive value of radiomics analysis of enhanced CT for three-tiered microvascular invasion grading in hepatocellular carcinoma. Med Phys 50: 6079-6095, 2023.
23. Roayaie S, Blume IN, Thung SN, Guido M, Fiel MI, Hiotis S, Labow DM, Llovet JM and Schwartz ME: A system of classifying microvascular invasion to predict outcome after resection in patients with hepatocellular carcinoma. Gastroenterology 137: 850-855, 2009.
24. Hwang YJ, Bae JS, Lee Y, Hur BY, Lee DH and Kim H: Classification of microvascular invasion of hepatocellular carcinoma: Correlation with prognosis and magnetic resonance imaging. Clin Mol Hepatol 29: 733-746, 2023.
25. Xu W, Li R and Liu F: Novel prognostic nomograms for predicting early and late recurrence of hepatocellular carcinoma after curative hepatectomy. Cancer Manag Res 12: 1693-1712, 2020.
26. Yang L, Gu D, Wei J, Yang C, Rao S, Wang W, Chen C, Ding Y, Tian J and Zeng M: A radiomics nomogram for preoperative prediction of microvascular invasion in hepatocellular carcinoma. Liver Cancer 8: 373-386, 2019.

27. Liu J, Cheng D, Liao Y, Luo C, Lei Q, Zhang X, Wang L, Wen Z and Gao M: Development of a magnetic resonance imaging-derived radiomics model to predict microvascular invasion in patients with hepatocellular carcinoma. Quant Imaging Med Surg 13: 3948-3961, 2023.
28. Zhang X, Ruan S, Xiao W, Shao J, Tian W, Liu W, Zhang Z, Wan D, Huang J, Huang Q, *et al*: Contrast-enhanced CT radiomics for preoperative evaluation of microvascular invasion in hepatocellular carcinoma: A two-center study. Clin Transl Med 10: e111, 2020.
29. Meng XP, Wang YC, Zhou JY, Yu Q, Lu CQ, Xia C, Tang TY, Xu J, Sun K, Xiao W and Ju S: Comparison of MRI and CT for the prediction of microvascular invasion in solitary hepatocellular carcinoma based on a non-radiomics and radiomics method: Which imaging modality is better? J Magn Reson Imaging 54: 526-536, 2021.
30. Wei JW, Jiang HY, Zeng MS, Wang MY, Niu M, Gu DS, Chong H, Zhang Y, Fu F, Zhou M, *et al*: Prediction of microvascular invasion in hepatocellular carcinoma via deep learning: A multi-center and prospective validation study. Cancers (Basel) 13: 2368, 2021.
31. Hirokawa F, Hayashi M, Miyamoto Y, Asakuma M, Shimizu T, Komeda K, Inoue Y and Uchiyama K: Outcomes and predictors of microvascular invasion of solitary hepatocellular carcinoma. Hepatol Res 44: 846-853, 2014.
32. An C, Rhee H, Han K, Choi JY, Park YN, Park MS, Kim MJ and Park S: Added value of smooth hypointense rim in the hepatobiliary phase of gadoxetic acid-enhanced MRI in identifying tumour capsule and diagnosing hepatocellular carcinoma. Eur Radiol 27: 2610-2618, 2017.
33. Kim KA, Kim MJ, Jeon HM, Kim KS, Choi JS, Ahn SH, Cha SJ and Chung YE: Prediction of microvascular invasion of hepatocellular carcinoma: Usefulness of peritumoral hypointensity seen on gadoxetate disodium-enhanced hepatobiliary phase images. J Magn Reson Imaging 35: 629-634, 2012.
34. Force M, Park G, Chalikonda D, Roth C, Cohen M, Halegoua-DeMarzio D and Hann HW: Alpha-fetoprotein (AFP) and AFP-L3 is most useful in detection of recurrence of hepatocellular carcinoma in patients after tumor ablation and with low AFP level. Viruses 14: 775, 2022.
35. Imura S, Teraoku H, Yoshikawa M, Ishikawa D, Yamada S, Saito Y, Iwahashi S, Ikemoto T, Morine Y and Shimada M: Potential predictive factors for microvascular invasion in hepatocellular carcinoma classified within the Milan criteria. Int J Clin Oncol 23: 98-103, 2018.
36. Liu W, Song K, Zheng W, Huo L, Zhang S, Xu X, Wang P and Jia N: Hepatobiliary phase features of preoperative gadobenate-enhanced mr can predict early recurrence of hepatocellular carcinoma in patients who underwent anatomical hepatectomy. Front Oncol 12: 862967, 2022.
37. Kumada T, Nakano S, Takeda I, Kiriyama S, Sone Y, Hayashi K, Katoh H, Endoh T, Sassa T and Satomura S: Clinical utility of *Lens culinaris* agglutinin-reactive alpha-fetoprotein in small hepatocellular carcinoma: Special reference to imaging diagnosis. J Hepatol 30: 125-130, 1999.
38. Miyaaki H, Nakashima O, Kurogi M, Eguchi K and Kojiro M: *Lens culinaris* agglutinin-reactive alpha-fetoprotein and protein induced by vitamin K absence II are potential indicators of a poor prognosis: A histopathological study of surgically resected hepatocellular carcinoma. J Gastroenterol 42: 962-968, 2007.
39. Wang MD, Sun LY, Qian GJ, Li C, Gu LH, Yao LQ, Diao YK, Pawlik TM, Lau WY, Huang DS, *et al*: Prothrombin induced by vitamin K Absence-II versus alpha-fetoprotein in detection of both resectable hepatocellular carcinoma and early recurrence after curative liver resection: A retrospective cohort study. Int J Surg 105: 106843, 2022.
40. Hu H, Zheng Q, Huang Y, Huang XW, Lai ZC, Liu J, Xie X, Feng ST, Wang W and Lu M: A non-smooth tumor margin on preoperative imaging assesses microvascular invasion of hepatocellular carcinoma: A systematic review and meta-analysis. Sci Rep 7: 15375, 2017.
41. Xu W, Wang Y, Yang Z, Li J, Li R and Liu F: New insights into a classification-based microvascular invasion prediction model in hepatocellular carcinoma: A multicenter study. Front Oncol 12: 796311, 2022.
42. Wang L, Feng B, Li D, Liang M, Wang S, Wang S, Ma X and Zhao X: Risk stratification of solitary hepatocellular carcinoma ≤5 cm without microvascular invasion: Prognostic values of MR imaging features based on LI-RADS and clinical parameters. Eur Radiol 33: 3592-3603, 2023.
43. Lee S, Kang TW, Song KD, Lee MW, Rhim H, Lim HK, Kim SY, Sinn DH, Kim JM, Kim K and Ha SY: Effect of microvascular invasion risk on early recurrence of hepatocellular carcinoma after surgery and radiofrequency ablation. Ann Surg 273: 564-571, 2021.
44. Jiang H, Wei H, Yang T, Qin Y, Wu Y, Chen W, Shi Y, Ronot M, Bashir MR and Song B: VICT2 trait: Prognostic alternative to peritumoral hepatobiliary phase hypointensity in HCC. Radiology 307: e221835, 2023.